DOUBLE FREQUENCY GENERATION IN NEODYMIUM-ACTIVATED LaF_3 CRYSTALS

A. M. PROKHOROV, V. A. SYCHUGOV, and G. P. SHIPULO

P. N. Lebedev Physics Institute, USSR Academy of Sciences

Submitted December 26, 1968

Zh. Eksp. Teor. Fiz. 56, 1806−1814 (June, 1969)

Theoretical analysis of double frequency generation in some Nd^{3+} doped crystals (LaF_3, mixed crystals, and $CaWO_4$) shows that, besides a definite ratio of laser transition probabilities, the principal condition of double frequency generation is a relatively low probability of the ${}^4I_{11/2} \to {}^4I_{9/2}$ (W_{21}) transition. The results of the analysis are confirmed by the study of the time characteristics of the output emission from a CaF_2-YF_3:Nd^{3+} laser at two frequencies. They are also confirmed by the study of thermal dependence of the generation threshold of the LaF_2:Nd^{3+} laser and of the saturation effect used as a basis of computing the value of $W_{21} \sim 10^4 - 10^5$ sec^{-1}.

LaF_3:Nd^{3+} crystals were first studied in[1,2]. It was established that it is possible to generate the lines λ_1 = 10,400 Å and λ_L = 10,630 Å with different thresholds. These lines correspond to transitions from the lower level of the ${}^4F_{3/2}$ term to two different levels of the ${}^4I_{11/2}$ term (see diagram in Fig. 1a). Line 1 has a lower threshold than line 2 in the temperature range near 77°K[1] or near 300°K[2]. An analogous phenomenon is observed in the case of mixed crystals (CaF_2-YF_3 and α-$NaCaYF_3$) doped with Nd^{3+}[3] ($\lambda_1 \approx$ 10,540 Å, $\lambda_2 \approx$ 10,630 Å, T ~ 300°K) and operating on the same principle (Fig. 1a), and in the case of $CaWO_4$:Nd^{3+} crystals that generate the lines $\lambda_1 \approx$ 10,580 Å and $\lambda_2 \approx$ 10,650 Å with different thresholds. The last two lines correspond to transitions from both levels of the term ${}^4F_{3/2}$ to the same level of term ${}^4I_{11/2}$ (Fig. 1b). The generation threshold of line 1 here is lower than that of line 2 at T = 295°K[4] and below down to ~203°K[5].

The observed phenomenon can be attributed to the fact that in the course of generation of line 1 the population of term ${}^4F_{3/2}$ increases with rising pump energy in accordance to the rising population of term ${}^4I_{11/2}$ because of the relatively low decay rate. Since the lower

FIG. 1. Double frequency generation schemes. a–for LaF_3 and mixed crystals activated with Nd^{3+} ($\lambda_1 = \lambda_{42}$, $\lambda_2 = \lambda_{43}$); b–for $CaWO_4$:Nd^{3+} ($\lambda_1 = \lambda_{42}$, $\lambda_2 = \lambda_{32}$).

level of transition 2 in scheme 1a is higher (or the upper level in scheme 1b is lower) than the corresponding level of transition 1 ($\Delta\nu_{32}$ = 206 cm^{-1} for LaF_3, $\Delta\nu_{32}$ = 80 cm^{-1} for mixed crystals, and $\Delta\nu_{43}$ = 63 cm^{-1} for $CaWO_4$) line 2 is also generated at some value of the pump energy. This also means that we should expect a delay in the onset of generation of line 2 relative to that of line 1.

Consequently the generation of two frequencies in LaF_3, in mixed crystals, and in $CaWO_4$, doped with Nd^{3+},

is completely explained by the low probability of the transition ${}^4I_{11/2} \to {}^4I_{9/2}$ as compared to the probability of relaxation between the levels within the terms ${}^4I_{11/2}$ and ${}^3F_{3/2}$.

ANALYSIS OF DOUBLE FREQUENCY GENERATION SCHEMES IN THE STATIONARY CASE

The analysis of the above phenomenon can be based on kinetic equations derived for a five-level scheme (Fig. 1a). These equations have the following form:

$$dN_1 / dt = N_2 W_{21} - (N_1 - N_5)B_{51}u_{51},$$
$$dN_2 / dt = (N_4 - N_2)B_{42}u_{42} + N_3 W_{32} - N_2(W_{21} + W_{23}),$$
$$dN_3 / dt = (N_4 - N_3)B_{43}u_{43} - N_3 W_{32} + N_2 W_{23},$$
$$dN_4 / dt = N_5 W_{54} - (N_4 - N_3)B_{43}u_{43} - (N_4 - N_2)B_{42}u_{42},$$

$$dN_5 / dt = -N_5 W_{54} + (N_1 - N_5)B_{51}u_{51},$$
$$N_0 = N_1 + N_2 + N_3 + N_4 + N_5,$$
$$du_{43} / dt = -\alpha_{43}u_{43} + B_{43}u_{43}h\nu_{43}(N_4 - N_3),$$
$$du_{42} / dt = -\alpha_{42}u_{42} + B_{42}u_{42}h\nu_{42}(N_4 - N_2). \tag{1}$$

Here N_i are the energy level populations, W_{ik} are probabilities of nonradiative transitions, B_{ik} are Einstein coefficients for stimulated transitions, u_{42} and u_{43} are radiation densities, and α_{42} and α_{43} are total losses in the optical resonator at the transitions frequencies ν_{42} and ν_{43}. Spontaneous emission and some nonradiative transitions were neglected in (1). In deriving these equations and in the subsequent analysis it is assumed that $W_{54} \gg B_{51}u_{51}$, and $W_{32} \gg W_{21}$.

We first consider the case of generation at the frequency ν_{42} ($\nu_{42} > \nu_{43}$). Here the stationary value of emission energy density u_{42} as a function of pumping is

$$u_{42} = u_{42}^* / \left[\frac{2W_{32} + W_{23}}{W_{32}} + \frac{W_{21}}{B_{51}u_{51}} \right], \tag{2}$$

where the value

$$u_{42}^* = \frac{W_{21}}{B_{42}} \left(\frac{N_0 h\nu_{42}B_{42}}{\alpha_{42}} - 1 \right)$$

is proportional to the limiting value of emission energy density in the resonator. Figure 2 shows a plot of u_{42} as a function of $B_{51}u_{51}$.

The possibility of generation at the frequency ν_{43} is determined by the nature of the variation of population difference between levels 4 and 3 depending on pumping. This difference is determined by the following formula:

$$\Delta N_{43} = N_0 \frac{B_{51}u_{51}[B_{42}u_{42}{}^*(W_{32} - W_{23}) + W_{21}(2W_{32} + W_{23})] + W_{21}{}^2\,W_{32}}{(B_{42}u_{42}{}^* + W_{21})[B_{51}u_{51}(2W_{32} + W_{23}) + W_{21}\,W_{32}]} \tag{3}$$

Analysis of (3) shows that ΔN_{43} increases with pumping (Fig. 2) so that under certain conditions the generation threshold can be reached at the frequency ν_{43}. The corresponding value of $B_{51}u_{51}$ is

$$(B_{51}u_{51})_{43}{}^{\text{th}} = \frac{(\xi B_{42} - B_{43})\,W_{21}\,W_{32}}{(N_0 h\nu_{13}\,\alpha_{43}{}^{-1}\,\xi B_{42} - 1)\,B_{43}\,(W_{32} - W_{23}) - (\xi B_{42} - B_{43})\,(2W_{32} + W_{23})} . \tag{4}$$

Here $\xi = \alpha_{43}\nu_{42}/\alpha_{42}\nu_{43}$ (practically $\xi \gtrsim 1$). If $\xi B_{42} - B_{43} > 0$, the quantity $(B_5 u_{51})_{43}{}^{\text{th}}$ is also larger than zero. This condition corresponds to our assumption that generation at the frequency ν_{42} occurs first. Consequently the above analysis shows that the decay rate of the lower laser level plays a significant role and can explain the experimentally observed phenomenon.
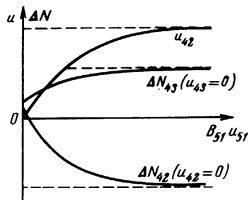
FIG. 2. u_{42}, ΔN_{43} at $u_{43} = 0$ and ΔN_{42} at u_{42} as functions of pump energy.

It is appropriate to investigate the case where generation at the frequency ν_{43} occurs first. The emission density function in the resonator then has a form similar to (2):

$$u_{43} = u_{43}{}^* \Big/ \Big[\frac{2W_{21} + 2W_{23} + W_{32}}{W_{32}} + \frac{W_{21}}{B_{51}\,u_{51}} \Big], \tag{5}$$

where

$$u_{43}{}^* = \frac{W_{21}}{B_{43}} \Big(\frac{N_0 h\nu_{43}\,B_{43}}{\alpha_{43}} - 1 \Big),$$

and the population difference between levels 4 and 2 is determined by

$$\Delta N_{42}$$
$$= N_0 \frac{B_{51}u_{51}[(2W_{21} + 2W_{23} + W_{32})\,W_{21} - B_{43}u_{43}{}^*(W_{32} - W_{23} - W_{21})] + W_{21}{}^2\,W_{32}}{(B_{43}u_{43}{}^* + W_{21})[B_{51}u_{51}(2W_{21} + 2W_{23} + W_{32}) + W_{21}\,W_{32}]} .$$

An analysis of this equation shows that ΔN_{42} decreases with pumping (Fig. 2). Thus if long-wave generation occurred first, no short-wave generation can take place in the stationary case.

We now consider the case when generation occurs simultaneously at two frequencies ν_{42} and ν_{43}. A stationary solution of (1) leads to the relation

$$(W_{32} - W_{23})u_{42} + \xi u_{43}(W_{32} - W_{23} - W_{21})$$
$$= W_{21}W_{32}(\xi B_{42} - B_{43}) / B_{42}B_{43}. \tag{6}$$

The consequences of this relation are, first, that generation of two frequencies is possible in the stationary case if $\xi B_{42} - B_{43} > 0$, i.e., generation at the frequency ν_{42} occurs first, and second, that an increase in emission density at one frequency causes a decrease of emission density at the other. The range of pump energies where double frequency generation is possible is determined by the expression

$$\Delta (B_{51}u_{51}) \approx \frac{\alpha_{42}W_{21}{}^2\,W_{32}(\xi B_{42} - B_{43})}{N_0 h\nu_{42}B_{42}B_{43}(W_{32} - W_{23})^2} , \tag{7}$$

the starting point of this range being determined by (4).

If all three above cases are summed up, the emission density in the resonator as a function of pumping $B_{51}u_{51}$
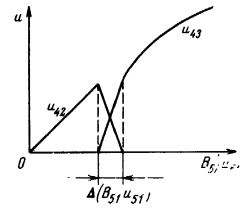
FIG. 3. u_{42} and u_{43} as functions of pump energy in the general case.

is schematically represented by the graph in Fig. 3.

Similar results can be obtained when a system of kinetic equations is solved for an energy level scheme in which the upper laser level has two components (Fig. 1b)[1]. The solution is obtained under the same conditions as in the case of Fig. 1a, except that $W_{21} \ll W_{43}$ instead of $W_{21} \ll W_{32}$. In this case the coupling between u_{42} and u_{32} has the form

$$u_{42}(W_{43} - W_{34}) + \xi u_{32}(W_{43} - W_{34} - W_{21}) = W_{21}\frac{\xi B_{42}W_{34} - B_{32}W_{43}}{B_{42}B_{32}} \tag{8}$$

where $\xi = \alpha_{32}\nu_{42}/\alpha_{42}\nu_{32}$. The generation of two frequencies is possible here if $\xi B_{42}W_{34} - B_{32}W_{43} > 0$. The range of pump energies in which simultaneous generation of the frequencies ν_{42} and ν_{32} is possible is approximately equal to

$$\Delta (B_{51}u_{51}) \approx \frac{\alpha_{42}(\xi B_{42}W_{34} - B_{32}W_{43})\,W_{21}{}^2}{N_0 h\nu_{42}B_{42}B_{32}(W_{43} - W_{34})^2} . \tag{9}$$

The starting point of this range corresponds to the generation threshold at the frequency ν_{32}:

$$(B_{51}u_{51})_{32}{}^{\text{th}} = W_{21}W_{34}(\xi B_{42}W_{34} - B_{32}W_{43}) \Big/ \Big[\Big(\frac{N_0 h\nu_{32}}{\alpha_{32}}\xi B_{42}W_{34} - W_{43} - W_{34} \Big) \cdot B_{32}(W_{43} - W_{34}) - (\xi B_{42}W_{34} - B_{32}W_{43})(W_{43} + 2W_{34}) \Big]. \tag{10}$$

In both energy level schemes the ratio of pumping range values allowing for the generation of both transitions to the pump energy corresponding to emission at the longer wavelength has the form

$$\frac{\Delta (B_{51}u_{51})}{(B_{51}u_{51})_{43}{}^{\text{th}}} \approx \frac{W_{21}}{W_{32}[1 - \exp(-\Delta\nu_{32}/kT)]} \tag{11a}$$

for the scheme in Fig. 1a, and

$$\frac{\Delta (B_{51}u_{51})}{(B_{51}u_{51})_{32}{}^{\text{th}}} \approx \frac{W_{21}}{W_{43}[1 - \exp(-\Delta\nu_{43}/kT)]} \tag{11b}$$

for the scheme in Fig. 1b.

If $W_{21} \ll W_{32}$ and $W_{21} \ll W_{43}$, then $\Delta(B_{51}u_{51})/(B_{51}u_{51})^{\text{th}} \ll 1$.

EXPERIMENTAL RESULTS

In our experiments we used $LaF_3 : Nd^{3+}$ crystals grown by the Stockbarger method and having a neodymium concentration of 1–2% by weight. These crystals generated lines 1 ($\lambda_1 \approx 10,400$ Å) and 2 ($\lambda_2 \approx 10,630$ Å) at T = 77°K and line 2 ($\lambda_2 \approx 10,633$ Å) only at T = 300°K. We studied the output energy as a function of pumping and generation threshold as a function of temperature in the pulse mode. In the first case a twin lamp elliptical reflector with separate power supply to the lamps was used to increase the pumping energy. To avoid saturation in the lamps, their load did not exceed 60% of the rated value. The measurements were performed at

_____

[1] The $CaWO_4$:Nd^{3+} laser operating according to the scheme in Fig. 1b generates two frequencies in the stationary case [5].

room temperature. In the second case we used a single-lamp elliptical reflector and the crystal was cooled with liquid nitrogen or its vapors[6]. In both cases the short-wave portion of the spectrum of the IFP-800 lamps was absorbed by the ZhS-17 filter to avoid the "aging" effect in crystals.

According to Fig. 4, an increase in pumping energy is accompanied by the effect of saturation of the output energy for various values of

$$\alpha = \frac{c}{2L} \ln \frac{1}{R_1 R_2},$$

where R_1 and R_2 are the mirror reflection coefficients. Using (5) and the measured relationships (Fig. 4) we can approximately evaluate the probability W_{21} assuming that $W_{21} \ll W_{32}$. This gives a value of $W_{21} \sim 10^4-10^5$ sec^{-1}.

To make this probability more precise we attempted to achieve monochromatic excitation of LaF$_3$:Nd^{3+} crystals with the ruby laser light. The laser emission was focused with a long-focus lens on the end face of the crystal (diameter 5 mm). The generation threshold of the crystal 50 mm long in a semi-confocal resonator with R = 95% was 1.9 J. The high value of the threshold was due to the weak absorption at the wavelength λ = 6943 Å (k = 0.124 cm^{-1}). The low strength of the LaF:Nd^{3+} crystals prohibits the use of high pumping energies (at 40—50 J of monochromatic pumping the crystals break down). Nevertheless the ruby laser can be used as a pump source for the LaF$_3$:Nd^{3+} crystals to investigate the characteristics of this material as well as of CaF$_2$:Dy^{2+}[7] and CaWO$_4$:Nd^{3+}[8].

The temperature dependence of the generation threshold of lines 1 and 2 (Fig. 5) was investigated for three LaF$_3$:Nd^{3+} crystals in the range 77—300°K. The crystals were grown without seeds and therefore had an arbitrary orientation of the optical axis (C) with respect to the axis of the active element (F) (i.e., with respect to the direction of radiation). In Fig. 5 curves 1 and 1', 2 and 2', and 3 and 3' correspond to crystals with angles between C and F of 30, 45, and 51°.

The study of polarization of the generation lines showed that the short-wave line has a preponderant π-polarization (the electric vector $\mathscr{E}$ is parallel to the CF plane) and the long-wave line has a σ-polarization ($\mathscr{E}$ is perpendicular to the CF plane).

Time characteristics of generation pulses were studied on CaF$_2$-YF$_3$:Nd^{3+} crystals (92% CaF$_2$, 6% YF$_3$,
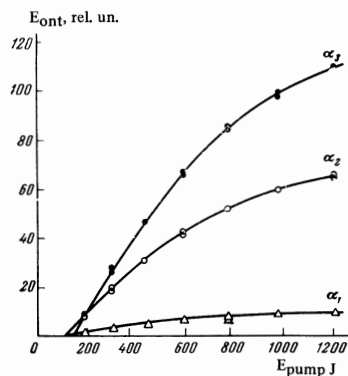
FIG. 4. Output energy of LaF$_3$:Nd^{3+} laser as function of pump energy for various α. $\alpha = 1.5 \times 10^7$ sec^{-1}, $\alpha_2 = 1.5 \times 10^8$ sec^{-1}, $\alpha_3 = 4.2 \times 10^8$ sec^{-1}.
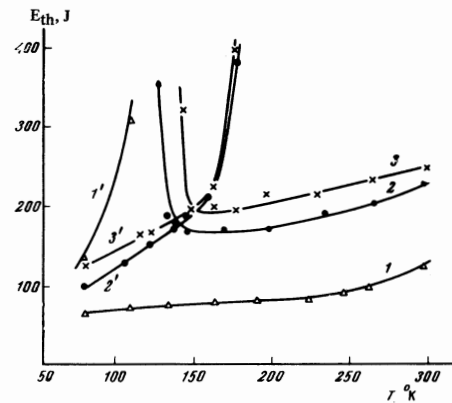
FIG. 5. Thermal dependence of threshold pump energy for LaF$_3$: Nd^{3+}. Curves 1', 2', and 3' for λ_1; curves 1, 2, and 3 for λ_2; 1' ≮ 1—≮(CF) = 30°, 2', 2—≮(CF) = 45°; 3', 3—≮(CF) = 51°.

2% NdF$_3$) that generated two frequencies at room temperature. The generation thresholds of lines 1 and 2 were 38 and 40 J respectively. The generation lines in the spectrum were picked up by two FÉU-28 photomultipliers placed at the output of the DFS-8 using special prisms. The oscilloscopic traces of pulses taken at various pumping energies (some are given in Fig. 6) show a delay in the start of generation of line 2 with respect to line 1 (Fig. 6a). As pumping energy is increased the generation threshold is reached in the initial stage of the pumping pulse where the slope is steep and thus the delay almost vanishes there (Fig. 6b and 6c). When the excess over threshold is considerable generation of line 1 is observed only in the beginning and at the end of the pumping pulse (Fig. 6c).

DISCUSSION OF RESULTS

It follows from (6) that the energy density of the short-wave radiation in the resonator may not exceed a certain definite value:

$$u_{42} \leqslant (\xi B_{42} - B_{43}) W_{21} W_{32} / B_{42} B_{43} (W_{32} - W_{23}).$$

Setting $B_{42} \approx 2 B_{43} = 2 \times 10^{10}$ cm^3/j·sec ($\sigma_{42} \approx 2 \times 10^{-19}$ cm^2), $W_{21} \approx 10^4-10^5$ sec^{-1}, and the reflection coefficient of the output mirror to equal 90%, we find that the limiting power of output emission at the higher frequency is $\sim 10^2-10^3$ W. In the pulse mode such powers can be reached at low pump energies (less than 100 J) as shown by the oscilloscopic traces in Fig. 6 for example.

The study of time characteristics of double frequency generation pulses confirms our assumptions stated at the beginning of this paper, and the results of analyzing the scheme of Fig. 1a presented in Fig. 3. In the first place, there is the delay of the start of long-wave generation relative to the short-wave generation that is most clearly observed at low pump excess over threshold (Fig. 6a), since the generation thresholds were similar for both frequencies. In the second place, as is apparent from comparing Fig. 6b and Fig. 6c, the energy of the short-wave component quickly reaches its limiting value with increasing pump energy, while the main portion of the total generation energy is emitted by the long-wave component, i.e., a "red shift" effect is observed[3].
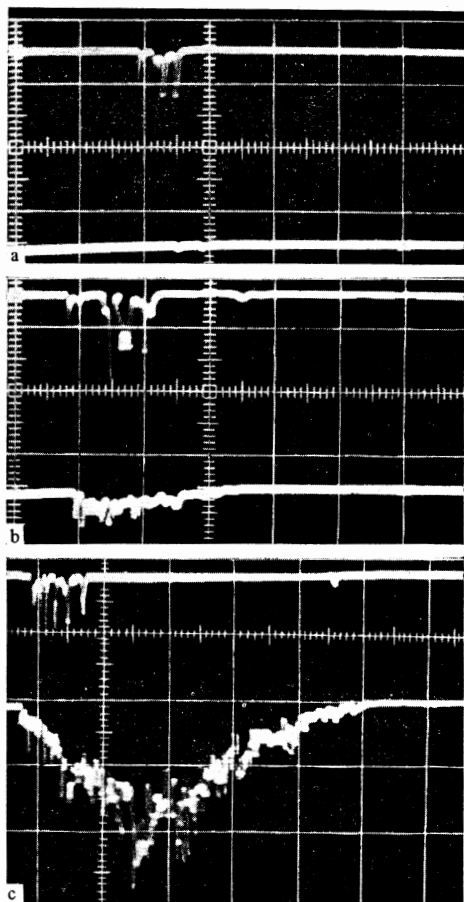
FIG. 6. Oscilloscopic traces of CaF_2-YF_3:Nd^{3+} laser generation (upper beam for λ_1 lower beam for λ_2) for various ratios p of pump energy to threshold energy. a–p = 1.5; b–p = 1.36; c–p = 2.8. Sweep 50 μsec/cm.

The results of the study of the "red shift" performed by Kaminskiĭ[3] also confirm our assumptions and conclusions. This is particularly evident in the case of yttrium fluorite crystals (see Fig. 3 in[3]): at first the entire generation energy falls on line B ($\lambda_B \approx 10{,}540$ Å) and then, after the generation threshold of line C ($\lambda_C \approx 10{,}632$ Å) is exceeded, energy is redistributed between lines B and C so that when $E_{pump} > 10E_{th}(B)$ the main portion of the energy falls on the C component. It was also noted in[3] that an analogous "red shift" effect is observed in KGSS and LGS glasses. It appears that the results of our analysis of double frequency generation schemes can be generalized to the case of continuous distribution of Stark components, as in glasses and liquids. This can provide the basis for a complete explanation of the shift towards the red of the intensity maximum in the generation spectrum. However even the above analysis provides a complete qualitative picture of this phenomenon.

LaF₃ crystals have a Debye temperature (T_D) of ~400°K[9] and thus the nonradiative transition from the lower level of term $^4I_{11/2}$ to the upper level of term $^4I_{9/2}$ ($\Delta\nu \approx 1700$ cm⁻¹) requires the participation of 6—7 phonons; this apparently is the reason for the relatively

low value of $W_{21} \approx 10^4$–10^5 sec⁻¹[2)] and for the associated effect of emission energy saturation with increasing pump energy. This conclusion seems to be valid also for mixed crystals with $T_D \sim 400°$K, i.e., in their case we should also observe the saturation effect in plotting the output energy as a function of pumping energy as long as the "red shift" effect is present.

It was noted in[11,12] that a minimum was observed in the curve of thermal dependence of the threshold in LaF₃:Nd^{3+} and some other crystals. The same sources attempt to relate the temperature of the minimum generation threshold T_m with T_D. Whlie in[11] T_m was found to lie in the range 400—450°K for LaF₃:Nd^{3+}, our measurements yield T_m values in the range 77—160°K (Fig. 5). This difference in T_m we ascribe to the difference in the angles between C and F of the investigated crystals. It seems that in[4] the crystal had $\sphericalangle$(CF) $\approx 90°$. Therefore the location of the threshold minimum has no direct relation to T_D. This concerns not only the LaF₃:Nd^{3+} crystals. We note that in the case of YAG:Nd^{3+} this minimum is observed at $T_m \approx 230°$K, while $T_D \approx 700°$K[6].

The analysis of data given in[6,12] shows that the minimum in the thermal dependence of the threshold is observed whenever generation occurs at two or more frequencies and always for the long-wave component. In cases when there is only one line we observe a smooth rise of the threshold with the temperature. This permits us to use our results for a qualitative explanation of some features of the thermal dependence of the generation threshold. In the first place as noted earlier, if generation occurs first at the frequency ν_{43}, the generation threshold cannot be reached at ν_{42} in the stationary case. Thus a rapid rise of this threshold with temperature in the pulse mode at $T > T_0$ is to be expected (T_0 is the temperature at which the generation thresholds at the frequencies ν_{42} and ν_{43} are equal).

The rise of the generation threshold at the frequency ν_{43} for $T < T_0$ can be understood with the aid of the formula determining the generation threshold at the frequency ν_{43} as a function of emission density at the frequency ν_{42}:

$$(B_{51}u_{51})_{43} = W_{21}W_{32}u_{42}B_{42} \bigg/ \bigg\{ \frac{B_{43}N_0 h\nu_{43}}{a_{43}}[B_{42}u_{42}(W_{32} - W_{23}) + W_{21}W_{32}]$$

$$- B_{42}u_{42}(2W_{32} + W_{23}) - W_{21}W_{32} \bigg\}. \qquad (12)$$

Insofar as the generation threshold at the frequency ν_{42} decreases when $T < T_0$, u_{42} increases faster with increasing pump energy and the generation threshold at the frequency ν_{43} increases according to (12). However the increase of u_{42} is limited by its nonlinear variation with increasing pump energy (see (2)). Therefore the generation threshold at the frequency ν_{43} can nevertheless be reached at a certain value of pump energy. Consequently the increase in generation threshold at the long-wave transition at $T < T_0$ is bound with the decrease of the threshold at the short-wave transition. Obviously the minimum of generation threshold will be observed at some temperature T_m close to T_0.

_____

[2)] In the case of Pr^{3+} in $LaCl_3$ theoretical computation yields the value of $W(3P_2 \rightarrow 3P_1) \approx 3 \times 10^4$ sec⁻¹ ($\Delta\nu \approx 1200$ cm⁻¹) [10].

The analysis of double frequency generation schemes and of the results of experimental research leads to the following conclusions.

1. Double frequency generation according to schemes of Figs. 1 a and 1 b is possible under two main conditions:

a. $W_{21} \ll W_{32}$, $\xi B_{42} > B_{43}$, scheme of Fig. 1 a;

b. $W_{21} \ll W_{43}$, $\xi B_{42}W_{34} > B_{32}W_{43}$, scheme of Fig. 1b.

2. The range of temperatures within which we can observe double frequency generation is determined first of all by the last inequalities above under conditions (a) and (b); therefore in the case of anisotropic crystals ($LaF_3 : Nd^{3+}$, $CaWO_4 : Nd^{3+}$) T_0 depends on the mutual orientation of C and F.

3. The minimum of the generation threshold in the temperature dependent function exists only in the region of double frequency generation.

4. In the case of $LaF_3 : Nd^{3+}$ we observe the effect of generation energy saturation with increasing pumping enabling us to evaluate the quantity $W_{21} \sim 10^4 - 10^5$ sec^{-1}. This value of W_{21} we ascribe to the low Debye temperature ($\sim 400°K$).

The authors thank M. V. Dmitruk and V. V. Osiko for furnishing the crystals for the research.

[1] L. F. Johnson, J. Appl. Phys. 34, 897 (1963).

[2] M. V. Dmitruk and A. A. Kaminskiĭ, Zh. Eksp. Teor. Fiz. 53, 874 (1967) [Sov. Phys.-JETP 26, 531 (1968)].

[3] A. A. Kaminskiĭ, ibid. 54, 1659 (1968) [27, 889 (1968)].

[4] L. F. Johnson, Quantum Electronics, Proceeding of the Third International Congress, Paris 2, Paris—New York, 1964, p. 1021.

[5] H. R. Alag, R. S. Horwath, and C. B. Zarowin, Appl. Opt. 4, 559 (1965).

[6] V. A. Sychugov and G. P. Shipulo, Fiz. Tverd. Tela 10, 2821 (1968) [Sov. Phys.-Solid State 10, 2224 (1969)].

[7] E. M. Zolotov, A. M. Prokhorov, and G. P. Shipulo, Zh. Eksp. Teor. Fiz. 49, 720 (1965) [Sov. Phys.-JETP 22, 498 (1966)]; Fiz. Tverd. Tela 10, 1071 (1968) [Sov. Phys.-Solid State 10, 848 (1968)].

[8] D. Röss and G. Zeidler, Z. Naturforsch. 21a, 336 (1966).

[9] W. M. Yen, W. C. Scott, and A. L. Schawlow, Phys. Rev. 136, A271 (1964).

[10] A. Kiel, Quantum Electronics, Proceedings of the Third Intern. Congress, Paris 1, Paris—New York, 1964, p. 765.

[11] A. A. Kaminskiĭ, ZhETF Pis. Red. 6, 615 (1967) [JETP Lett. 6, 115 (1967)].

[12] A. A. Kaminskiĭ, Zh. Eksp. Teor. Fiz. 54, 727 (1968) [Sov. Phys.-JETP 27, 388 (1968)].